# SUPPLEMENTARY INFORMATION
# Quantitative dynamic microscopy through scattering media without image reconstruction: a tool for biomedical optics

Matteo Brizioli[1], Roberto Cerbino[2], Fabio Giavazzi[1]

[1*]Dipartimento di Biotecnologie Mediche e Medicina Traslazionale, Università degli Studi di Milano, Via Fratelli Cervi 93, Segrate, 20054, Italy.

[2]Faculty of Physics, University of Vienna, Boltzmanngasse 5, Vienna, 1090, Austria.

**Supplementary Movie SM1** - Representative microscopy image sequence of diluted colloidal particles ($R = 0.5$ µm). Real-time duration is 50 $s$, the size of the image corresponds to 333 µm.

**Supplementary Movie SM2** - Representative microscopy image sequence of diluted colloidal particles ($R = 0.5$ µm) behind a Parafilm layer of thickness $L = 250$ µm, placed at a distance $z = 250$ µm from the sample. Real-time duration is 50 $s$, the size of the image corresponds to 333 µm.

**Supplementary Movie SM3** - Representative microscopy image sequence of whole blood flowing in a microfluidic channel. Real-time duration is 50 $s$, the size of the image corresponds to 333 µm.

**Supplementary Movie SM4** - Representative microscopy image sequence of whole blood flowing in a microfluidic channel behind a Parafilm layer of thickness $L = 375$ µm, placed at a distance $z = 180$ µm from the sample. Real-time duration is 50 s, the size of the image corresponds to 333 µm.

# Supplementary Note 1: Derivation of Eq. (10) of the main text

In this section, we provide a detailed derivation of the expression reported in Eq. (10) of the main text for the image structure function $D(\mathbf{q},\tau)$ in the presence of a turbid layer. We consider for simplicity the case of a single point-like particle in the object plane, whose position over time we indicate with $\mathbf{x}(t)$. Given the linearity of the imaging process, the generalization to the case of a collection of independent particles is straightforward. Using Eq. 7 of the main text, we can write the product of the Fourier-transformed images acquired at time $t$ and $t+\tau$, respectively, as

$$\begin{aligned}\hat{I}(\mathbf{q},t+\tau)\hat{I}^*(\mathbf{q},t) = \\ = \int d\mathbf{y_1}\mathcal{T}(\mathbf{x}(\mathbf{t}+\tau),\mathbf{y_1})\mathrm{e}^{-j\mathbf{q}\cdot\mathbf{y_1}} \times \int d\mathbf{y_2}\mathcal{T}(\mathbf{x}(\mathbf{t})+\Delta\mathbf{x},\mathbf{y_2})\mathrm{e}^{j\mathbf{q}\cdot\mathbf{y_2}} = \\ = \int d\mathbf{y}\int d\mathbf{r}\mathcal{T}(\mathbf{x}_0,\mathbf{y})\mathcal{T}(\mathbf{x}_0+\Delta\mathbf{x},\mathbf{y}+\mathbf{r})\mathrm{e}^{-j\mathbf{q}\cdot\mathbf{r}},\end{aligned} \tag{S1}$$

where $\Delta\mathbf{x} = \mathbf{x}(t+\tau) - \mathbf{x}(t)$ is the particle displacement from time $t$ to $t+\Delta t$ and $\mathbf{x}_0 = \mathbf{x}(t)$ its initial position. According to Eq. S1, the expectation value $\langle\hat{I}(\mathbf{q},t+\tau)\hat{I}^*(\mathbf{q},t)\rangle_{\mathbf{x_0}}$ of $\hat{I}(\mathbf{q},t+\tau)\hat{I}^*(\mathbf{q},t)$ over the (uniformly distributed) initial position of the particle $\mathbf{x}_0$ is proportional to the spatial Fourier transform with respect to $\mathbf{r}$ of the function:

$$\int d\mathbf{y}\int d\mathbf{x_0}\mathcal{T}(\mathbf{x}_0,\mathbf{y})\mathcal{T}(\mathbf{x}_0+\Delta\mathbf{x},\mathbf{y}+\mathbf{r}).$$

Using the expression in Eq. 1 of the main text for the transmission kernel $\mathcal{T}(\mathbf{x},\mathbf{y})$, we can expand the integrand as the product of two statistically independent terms (i) and (ii)

$$\begin{aligned}\mathcal{T}(\mathbf{x}_0,\mathbf{y})\mathcal{T}(\mathbf{x}_0+\Delta\mathbf{x},\mathbf{y}+\mathbf{r}) = \\ = \underbrace{\mathcal{T}_0(\mathbf{x}_0-\mathbf{y})\mathcal{T}_0(\mathbf{x}_0-\mathbf{y}+(\Delta\mathbf{x}-\mathbf{r}))}_{\text{(i)}} \times \\ \times \underbrace{[1+u(\mathbf{x}_0,\mathbf{y})+u(\mathbf{x}_0+\Delta\mathbf{x},\mathbf{y})+u(\mathbf{x}_0,\mathbf{y})u(\mathbf{x}+\Delta\mathbf{x},\mathbf{y})]}_{\text{(ii)}}.\end{aligned} \tag{S2}$$

The integral over $\mathbf{x_0}$ and $\mathbf{y}$ of the first term $(i)$ in Eq. S2 is given, up to a multiplicative constant, by

$$\int d\mathbf{x}_0\int d\mathbf{y}\ \text{(i)}\ = \int d\mathbf{x}'\int d\mathbf{y}'\mathcal{T}_0(\mathbf{y}')\mathcal{T}_0(\mathbf{y}'+(\Delta\mathbf{x}-\mathbf{r})) \propto C_P(\Delta\mathbf{x}-\mathbf{r}), \tag{S3}$$

$C_P(\mathbf{r})$ being the auto-correlation function of the average intensity profile $\mathcal{T}_0$ of the transmission kernel.

Using Eqs. 8 and 9 of the main text, the integral over $\mathbf{x_0}$ and $\mathbf{y}$ of the second term (ii) in Eq. S2 can be calculated as

$$\int d\mathbf{x}_0 \int d\mathbf{y}\ \text{(ii)}\ \propto 1 + u_0 c_a\left(\frac{\Delta x + \mathbf{r}}{2}\right) c_b(\Delta\mathbf{x} - \mathbf{r}) \tag{S4}$$

Combining Eqs.S2,S3 and S4 we get

$$\begin{aligned}
&\langle \hat{I}(\mathbf{q}, t+\tau)\hat{I}^*(\mathbf{q}, t)\rangle_{\mathbf{x}_0} \propto \\
&\qquad \propto \int d\mathbf{r} \mathrm{e}^{-j\mathbf{q}\cdot\mathbf{r}} C_P(\Delta\mathbf{x} - \mathbf{r})[1 + u_0 c_a\left(\frac{\Delta x + \mathbf{r}}{2}\right) c_b(\Delta\mathbf{x} - \mathbf{r})] = \\
&\qquad = \mathrm{e}^{-j\mathbf{q}\cdot\Delta\mathbf{x}} |\hat{\mathcal{T}}_0(\mathbf{q})|^2 + \int d\mathbf{r} \mathrm{e}^{-j\mathbf{q}\cdot\mathbf{r}} C_P(\Delta\mathbf{x} - \mathbf{r}) u_0 c_a\left(\frac{\Delta x + \mathbf{r}}{2}\right) c_b(\Delta\mathbf{x} - \mathbf{r}),
\end{aligned} \tag{S5}$$

where, according to the Wiener–Khintchin theorem, $|\hat{\mathcal{T}}_0|^2 = \mathcal{F}[C_p]$.

We note that the correlation function $c_b(\mathbf{r})$, which captures the characteristic fluctuation length of the speckle pattern, is much narrower than $C_P(\mathbf{r})$, whose decay length reflect the width of the average intensity profile $\mathcal{T}_0$. Adopting the approximation $u_0 C_P(\Delta\mathbf{x} - \mathbf{r}) c_b(\Delta\mathbf{x} - \mathbf{r}) \simeq \alpha c_b(\Delta\mathbf{x} - \mathbf{r})$, Eq. S5 becomes :

$$\begin{aligned}
&\langle \hat{I}(\mathbf{q}, t+\tau)\hat{I}^*(\mathbf{q}, t)\rangle_{\mathbf{x}_0} \propto \\
&\qquad \propto \int d\mathbf{r} \mathrm{e}^{-j\mathbf{q}\cdot\mathbf{r}} c_a\left(\frac{\Delta x + \mathbf{r}}{2}\right) c_b(\Delta\mathbf{x} - \mathbf{r}) = \\
&\qquad = \int d\mathbf{q}'\ \mathrm{e}^{-j(\mathbf{q}-\mathbf{q}')\cdot\Delta\mathbf{x}}\ \hat{c}_a(\mathbf{q}')\hat{c}_b(2\mathbf{q} - \mathbf{q}').
\end{aligned} \tag{S6}$$

If we now take the expectation value of both sides of Eq. S6 over the displacement $\Delta\mathbf{x}$, we get

$$\begin{aligned}
&\langle \hat{I}(\mathbf{q}, t+\tau)\hat{I}^*(\mathbf{q}, t)\rangle_{\mathbf{x}_0,\Delta\mathbf{x}} \simeq \\
&\qquad \simeq \langle\ \mathrm{e}^{-j\mathbf{q}\cdot\Delta\mathbf{x}}\rangle_{\Delta\mathbf{x}} |\hat{\mathcal{T}}_0(\mathbf{q})|^2 + c\int d\mathbf{q}' \langle\ \mathrm{e}^{-j(\mathbf{q}-\mathbf{q}')\cdot\Delta\mathbf{x}}\rangle_{\Delta\mathbf{x}} \hat{c}_a(\mathbf{q}')\hat{c}_b(2\mathbf{q} - \mathbf{q}') = \\
&\qquad = f(\mathbf{q}, \tau)|\hat{\mathcal{T}}_0(\mathbf{q})|^2 + \mathrm{c}\int d\mathbf{q}' f(\mathbf{q} - \mathbf{q}', \tau)\hat{c}_a(\mathbf{q}')\hat{c}_b(2\mathbf{q} - \mathbf{q}')
\end{aligned} \tag{S7}$$

where $f(\mathbf{q}, \tau) = \langle \mathrm{e}^{-j\mathbf{q}\cdot\Delta\mathbf{x}}\rangle$ is the ISF and $c$ is a constant. Considering the simple case of diffusive scattering particles, the ISF is given by $f(q, \tau) = \exp(-D\tau q^2)$, where $D$ is the diffusion coefficient. Therefore, for a given lag time $\tau$, the ISF decays as a function of $q$ with a characteristic relaxation wavevector $\frac{1}{\sqrt{D\tau}}$, while $\hat{c}_b(q)$ relaxes with a characteristic relaxation wavevector, which is inversely proportional to the speckle size $l_0$. In our experimental condition, the speckle size is always much smaller compared to the probed displacement $\frac{1}{\sqrt{D\tau}} \ll \frac{1}{l_0}$ implying that $q \simeq q'$. Therefore, we can write $f(\mathbf{q} - \mathbf{q}', \tau)\hat{c}_b(2\mathbf{q} - \mathbf{q}') \simeq f(\mathbf{q} - \mathbf{q}', \tau)\hat{c}_b(\mathbf{q})$. Performing this substitution in Eq. S7 we finally get

$$\langle \hat{I}(\mathbf{q}, t+\tau)\hat{I}^*(\mathbf{q}, t)\rangle \simeq f(\mathbf{q}, \tau)|\hat{\mathcal{T}}_0(\mathbf{q})|^2 + \alpha\hat{c}_b(\mathbf{q}) f(\mathbf{q}, \tau) * \hat{c}_a(\mathbf{q}) \tag{S8}$$

where $*$ indicates the convolution product. Using the identity $D(q,\tau) = 2\langle|\hat{I}(\mathbf{q},t)|^2\rangle - 2\Re\{\langle\hat{I}(\mathbf{q},t+\tau)\hat{I}^*(\mathbf{q},t)\rangle\}$ Eq. 10 of the main text immediately follows.

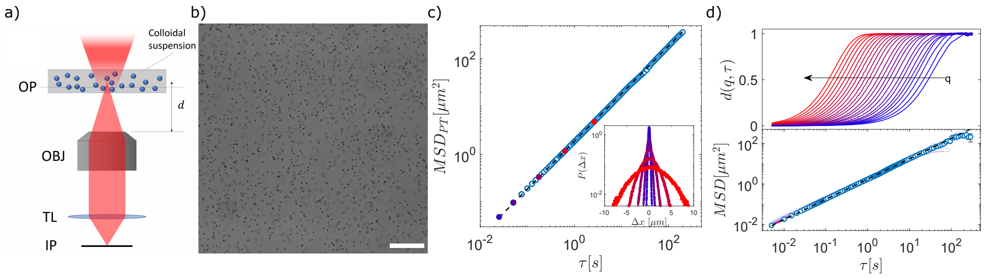


**Fig. S1 Experimental setup and quantification of Brownian dynamics.** a) Schematic representation of the essential elements of the microscopy setup (not in scale). The sample (a diluted colloidal suspension confined in glass capillary) is illuminated by an incoherent light beam generated by the microscope halogen lamp. The light scattered by the particles is collected by the microscope objective (OBJ). A tube lens (TL) forms an image of the object plane (OP) on the camera sensor (image plane, IP). (b) Representative bright-field image of the sample, the scale bar corresponds to 50 µm. (c) Empty circles: mean square particle displacement computed using SPT. Full circles coincide with the delay times whose PDFs are shown in the inset with the same color code. The black dashed line represents the best fitting curve of the $MSD$ with a linear model $MSD_{PT}(\tau) = 4D_{PT}\tau$, with $D_{PT} = 0.45 \pm 0.02$ µm$^2$/$s$. (d) Upper panel: representative normalized image structure functions (NISFs) obtained from DDM analysis for different wave vectors $q$ ranging from 0.2 µm$^{-1}$ (blue) to 3.8 µm$^{-1}$ (red). In the lower panel, the MSDs of the particles obtained from the inversion of the NISFs shown in the upper panel are reported as transparent lines, with the same color code used in the upper panel. The black dashed line corresponds to the best fitting curve $MSD_s(\tau) = 4D_s\tau$, with $D_s = 0.44 \pm 0.01$ µm$^2$/s, the DDM diffusion coefficient measured without the scattering layer.

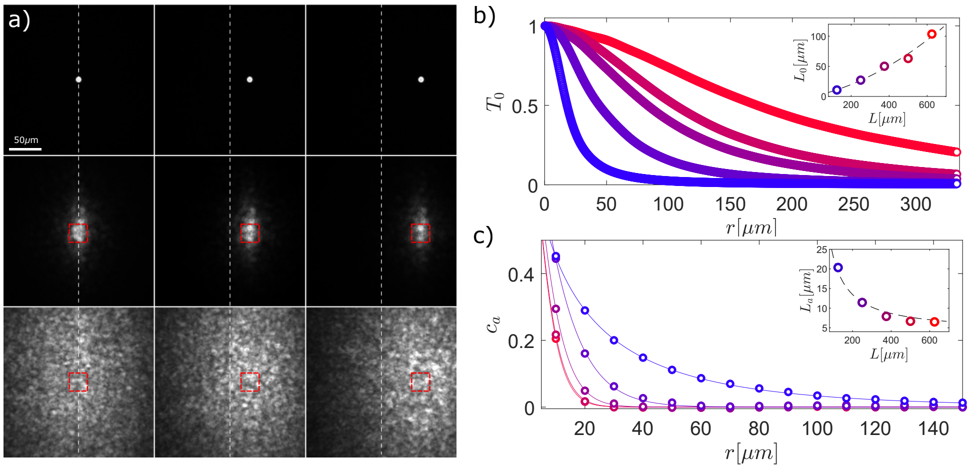


**Fig. S2 Experimental determination of the transmission kernel**. (a) A rigidly translating pinhole is imaged without any scattering layer (top row), in the presence of a Parafilm layer of thickness 250 µm (center row) and 500 µm (bottom row). Red squares indicate the instantaneous center of mass of the images, and the vertical white dashed lines are drawn in correspondence to the initial position of the pinhole. The size of each panel is 230 µm. (b) Azimuthally averaged intensity profile of the images of the pinhole, collected through Parafilm layers of different thicknesses ranging from 125 µm (blue) to 625 µm (red), placed at a fixed distance $z = 250$ µm from the sample. In the inset, the estimated width $L_0$ of the profile is plotted as a function of the layer thickness $L$ with the same color code. The black dashed line represent the best fit to $L_0(L)$ with the model $L_0 = \alpha z_0 L$, where $z_0 = z + L/2$ is the distance from the is the distance between the object plane and the center of the turbid layer, leading to $\alpha \simeq 2.8 \cdot 10^{-4}$ µm$^{-1}$. (c) Spatial correlation function $c_a(r)$ (see main text for details) for different layer thicknesses (same of (b)). The corresponding correlation length $L_a$, which identifies the length scale over which the imaging system is space-invariant, is reported in the inset as a function of the thickness $L$. The black dashed line is the best fitting curve to $L_a$ with a model $L_a = \epsilon z_0/L$, leading to $\epsilon \simeq 7.7$ µm

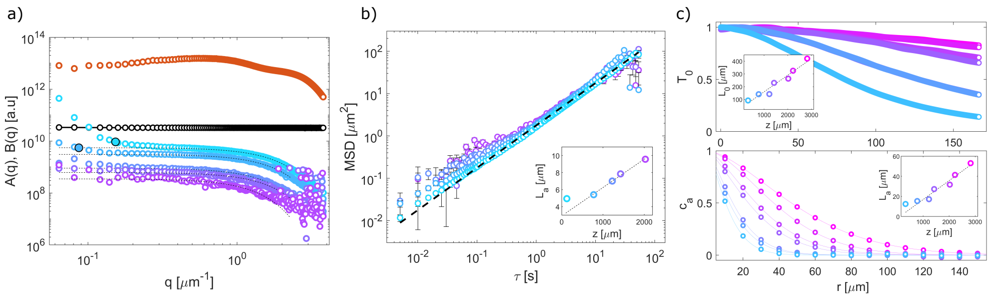


**Fig. S3** Results for different distances $z$ between the sample and a scattering layer of thickness $L = 375$ µm ranging from $z = 250$ µm (Cyan) to $z = 2900$ µm (pink). (a) Scattering amplitudes $A(q)$ for the acquisitions where the signal could be discriminated from the Noise $B(q)$ (black symbols). Red circles represent the scattering amplitude for the sample without any scattering layer and large filled circles correspond to the values of $q_{co}$. (b) Inverted MSDs from the normalized image structure functions $d(q, \tau)$ with black dashed line representing $MSD(\tau) = 4D_0\tau$ with $D_0$ computed using the Stokes-Einstein relation. In the Inset, the correlation length $L_a$ estimated from the optimization parameter $q_a$ as a function of $z$ The black dashed line is the best fit to $L_a$ with a linear model. (c) (Top plot) Average intensity profile $\mathcal{T}_0$ as a function of the distance $r$. In the inset, the size of the PSF $L_0$ is plotted as a function of the distance $z$. The black dashed line is the best fit to $L_0(z)$ using a linear model $L_0 = \alpha z_0 L$, yielding to $\alpha \simeq 3.5 \cdot 10^{-4}$ µm$^{-1}$. (Bottom plot) Correlation functions $c_a(r)$ for different $z$. The resulting $L_a$ as a function of the distance $z$ are shown in the inset. The black dashed line represent the best fit to $L_a$, with $L_a = \epsilon z_0/L$, leading to $\epsilon \simeq 6.5$ µm. The real-space characterization of the intensity profile and correlation function has been performed using a 40X, 0.60 NA objective.

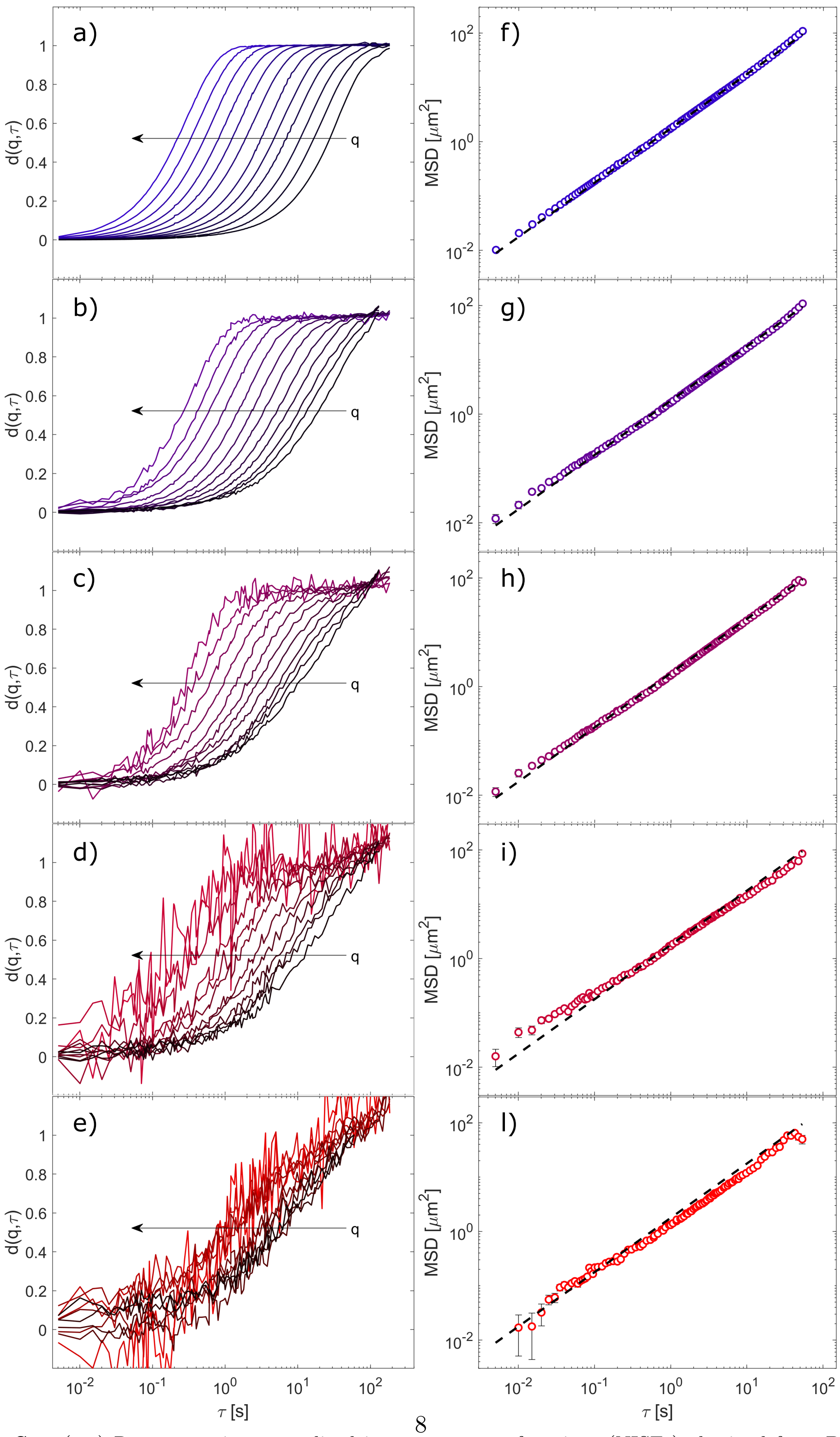




**Fig. S4** (a-e) Representative normalized image structure functions (NISFs) obtained from DDM analysis of diluted suspension of 0.5 µm particles for different thicknesses $L$ of the scattering layer, with $L$ ranging from 125 µm (a) to 625 µm (e) in steps of 125 µm. The considered $q$-range corresponds to [0.23 2.8] µm$^{-1}$. (f-l) Mean square displacements extracted from the corresponding NISFs using Eq. 11 of the main text in combination with the self-consistent algorithm described in the main text.

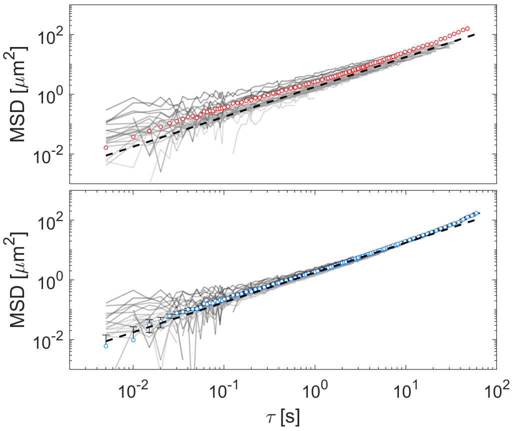


**Fig. S5** Comparison of the MSD extracted from the analytic inversion Eq. 6 of the main text (top plot) and the one exploiting the DDM-modified algorithm (Eq. 11) for diffusive particles placed behind a scattering layer of thickness $L = 375$ µm. Gray lines represent a "bundle" of MSDs estimated for different $q$-values in the range $[0.2 - 2]$ $\mu m^{-1}$. Colored symbols represent the MSD obtained as the average of the curves for all $q$ values. The black dashed lines are the theoretical predictions for $MSD(\tau) = 4D_0\tau$, with $D_0$ computed from the Stokes-Einstein relation.

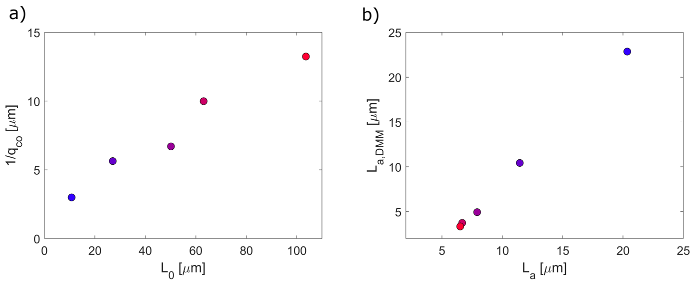


**Fig. S6** Comparison between the inverse of the cross-over wavevector $q_{co}$ (a) and $L_a$ (b) estimated from the reciprocal space analysis (DDM) with $L_0$ and $L_a$ obtained from the direct space characterization of the point-spread function of the optical system. The different colors correspond to different thicknesses of the Parafilm layer, ranging from 125 µm (blue) to 625 µm (red) in steps of 125 µm.

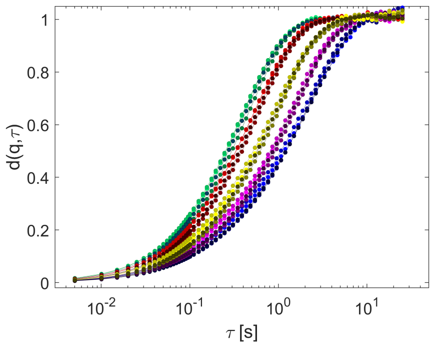


**Fig. S7** Comparison of the normalized image structure functions $d(q, \tau)$ of the diffusive sample behind a Parafilm layer of thickness $L = 125$ µm for $q = 0.95$ µm$^{-1}$(green), $q = 1.16$ µm$^{-1}$(red), $q = 1.46$ µm$^{-1}$ (yellow), $q = 1.92$ µm$^{-1}$ (violet) and $q = 2.25$ µm$^{-1}$ (blue) obtained using objectives with different magnification 10X (0.25 NA), 20X (0.45 NA), 40X (0.60 NA) and 60X (0.70 NA) from the darkest to the brightest one for each color, respectively.

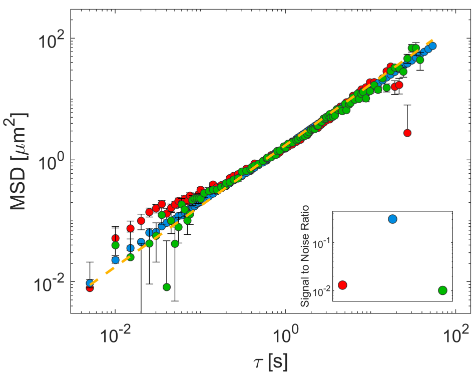


**Fig. S8** Inverted Mean squared displacement for the diffusive sample behind a tracing paper sheet (red), ground glass (blue) and a 1-mm thick slice of chicken breast (green). The yellow dashed line represents the theoretical prediction for the MSD using the Stokes-Einstein relation. In the inset, it is shown the signal-to-noise ratio for the three configuration with the same color code.

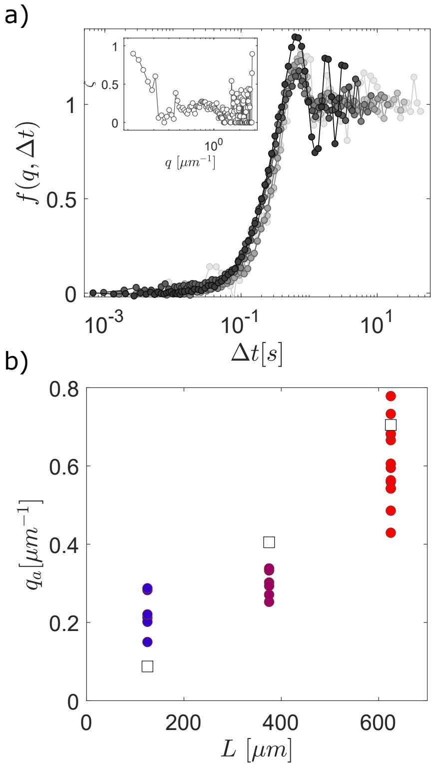


**Fig. S9** (a) Representative normalized image structures function of the blood flowing with velocity $v_0 = 5.2 \pm 0.4$ µm/s behind a Parafilm layer of thickness $L = 375$ µm plotted as a function of the scaled time $q\tau$ for different values of $q$ in the range $[0.2 - 1.7]$ µm$^{-1}$ (from dark to light gray). In the inset, the relative amplitude parameter $\zeta(q)$ obtained from the best fit to $d(q,\tau)$ with the model of Eq. (12) of the main text is shown. (b) Estimate of the memory effect range $q_a$ as a function of the parafilm thicknesses $L$, respectively 125 µm (blue), 375 µm (violet) and 625 µm (red). Colored circles represent the estimate obtained by fitting the data of the flowing blood to Eq. 12 of the main text, while empty squares represent the estimates obtained from the Brownian dynamics using the DDM-modified algorithm Eq. 11 in the main text.